Convergence of Varied Surrogate Models for Seismic Dynamic PRA/PSA

Brian Cohn*[a], Jieun Hur[b], Richard Denning[a], Tunc Aldemir[a], Halil Sezen[b]
[a] *Department of Mechanical and Aerospace Engineering, The Ohio State University Columbus, United States of America*
[b] *Department of Civil, Environmental and Geodetic Engineering, The Ohio State University Columbus, United States of America*

*cohn.72@osu.edu

Abstract: Surrogate models (SMs) describe a category of methods to approximate the response of a computer model based on a number of training runs. SMs allow analysts to more rapidly determine the impact of uncertainties on the system figures of merit of interest than sampling uncertainties on full computer models (FCM), as SMs are less complex than the models they are trained to approximate. However, it can prove challenging to make the determinations of which SM structure to use. A procedure is presented for demonstrating the applicability of different SMs for a given FCM and their convergence using a limited amount of training data.

Keywords: Surrogate Models, Seismic PRA, Dynamic PSA

1. INTRODUCTION

Surrogate models (SMs) are a category of methods to approximate the response of a computer model based on a number of training runs. SMs allow to more rapidly determine the impact of probabilities and uncertainties on the system figures of merit of interest than sampling uncertainties on many full computer models (FCMs), as SMs are less complex than the models they are trained to approximate. This paper illustrates a method to mechanistically determine the SM with the least bias among several possible SMs for seismic dynamic probabilistic risk/safety analysis (PRA/PSA). Section 1.1. provides a short background, Section 1.2. describes previous work on done by The Ohio State University (OSU) on this topic generating the seismic stick models used in this paper and exploring the use of SMs to approximate the full response. Section 1.3 lists outstanding research issues being addressed and presents the paper organization.

1.1. Background

The U.S. Department of Energy has established the Light Water Reactor Sustainability Program in order to maintain the existing nuclear reactor fleet beyond the original licenses of the plants. The Risk Informed Safety Margin Characterization (RISMC) pathway was developed as part this program to develop advanced methods to quantify risk in the operation of nuclear power plants (NPPs).

The OSU has recently completed a project under the RISMC pathway for the development of framework and tools to perform a systematically-integrated and verifiable internal/external events PRA/PSA, with a focus on investigation of common cause failures and consideration of the dynamic nature of seismic events. The uncertainty quantification work conducted within the project has been performed using the Idaho National Laboratory-developed Multiscale Object-Oriented Simulation Environment (MOOSE)[1].

The SM generation and sampling was performed using the Risk Analysis Virtual ENvironment (RAVEN) code [2] produced by Idaho National Laboratory. The RAVEN code is developed within the RISMC pathway and has capability to construct a wide variety of different SMs, each with its own set of tuning parameters. Because of the large number of options for SMs to use in an analysis, it is difficult to determine what form of which SM is the most accurate for a given scenario.

1.2. Previous Work

One component of the OSU project was the development of analysis tools for the uncertainty quantification of seismic computer models. SMs have been selected as a method of performing advanced uncertainty quantification due to the long run times of FCMs and various SM options have been examined through a number of case studies to date.

For each case study, a FCM was constructed to identify the probabilities of failure for two essentially identical nonstructural components (NSCs) located on different levels of a nuclear plant's auxiliary building, using uncertainty distributions for the mass and stiffness of the structure at each level [3]. SMs were trained on several runs of the FCM and used to predict the response of the overall system [4]. From this study, it was determined that the probabilities of failure predicted by the SMs could match the probabilities of failure from the FCMs while using fewer training points than the FCM used. However, the choice of the SM had a large effect on the difference between the SM and the FCM.

A followup study [5] was conducted to investigate the applicability of different SM construction algorithms to predict phenomena that were previously found to have a substantial effect on the predicted seismic response. This study used a set of common SM algorithms, selected without any prior knowledge of their applicability for the case under consideration. Two sets of data from the FCM were used to train the SMs, which then predicted the NSC failure probability on both floors of a 2-story auxiliary building. One set of training data was a low-fidelity set, consisting of 500 samples. The other set was a high-fidelity set and had 20,000 samples, and the relative error of each SM was calculated for both sets of training data.

1.3 Overview of the Proposed Approach

The followup case study led a procedure to determine the SM with the least model bias. It found that the relative error of a SM trained using Latin hypecube samples (LHSs) of the original FCM was similar regardless of the number of training points used. Therefore, by using a small number of training runs, a choice about the fitness of different SMs can be made. As different SMs may need different sampling strategies, being able to make a decision about SM selection sooner can reduce simulation time.

In general, the accuracy of a SM is gauged by comparing its results to the results obtained from the FCM whose runs could be quite time consuming. This paper presents a method to determine the applicability of different SMs without the need for such a comparison. The results of analysis are split into two different sets of information: the Full Set (FS) and the Analyst Set (AS). In FS, runs with the FCM are performed to determine the probability of failure of NSCs. Using the FS data, each of the candidate SMs is trained and then sampled for comparisons (Section 3.3). The results from the FCM and SMs are compared to identify the most accurate SM with the fewest training runs (Section 3.3).

The AS represents a more limited state of knowledge that more closely corresponds to the methodology that would be used in an industrial setting, where it is not feasible to perform a FS analysis. In this case, a reduced amount of information is gathered. First, a small number of training runs are used to train many candidate SMs. These candidate SMs are sampled with high fidelity to determine their error relative to the probability of failure obtained using the AS (Section 3.2). The candidate models which show a large error are removed from consideration and the number of training runs used is increased. This process is repeated until a single candidate SM is identified as having converged to the least error among all candidate SMs.

Section 2 describes the details of the methodology. Section 3 presents the results of the FCM and SM analyses and the results are discussed in Section 4.

2. METHODOLOGY

In this section, the computer models used in the analysis are described in Section 2.1, the mathematical descriptions of the SMs analyzed are given in Section 2.2 and the analysis steps performed are presented in Section 2.3.

2.1. Scenario Description

The seismic model consists of two essentially-identical NSCs belonging to independent trains of a safety-related system. These NSCs are located on different stories of the auxiliary building of a NPP. Figure 1 shows the structure of the auxiliary building and a representative stick model tuned to provide the same response as the three dimensional structure.

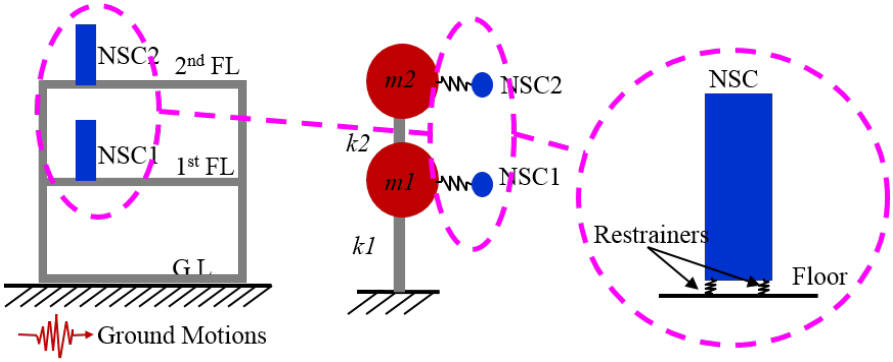

Fig.1. Simplified stick model is shown in the middle for seismic analysis of the structure and NSCs [3].

The stick model representation has a total of four parameters: m1 and m2, respectively, are the masses of the first and second floors of the structure, and k1 and k2, respectively, are the stiffnesses of each floor, which depend on the building materials and floor layout. This stick model was subjected to a set of ground motions (GMs) and the peak accelerations of both NSCs were recorded.

Simultaneously, failure accelerations for NSCs were taken from publicly-available failure data for DC battery racks installed at Zion Nuclear Power Plant [6]. The failure data were fitted to a log-normal distribution and sampled alongside each analysis of the stick model to determine the success or failure of the NSCs (see Table 1). For this analysis, both NSCs were treated as fully-identical and one failure acceleration was applied to the NSCs on both floors.

Table 1. Distribution parameters for analyses of stick model [3].

	Distribution	Mean	St. Dev.
Each floor mass m_1 and m_2 (ton)	Normal	25	2.5
Floor stiffness k_1 and k_2 (kN/m)	Normal	150,000	15,000
Failure acceleration (g)	Log-normal	1.01	0.69

2.2. SM Implementation

Consider a time-dependent model that can be represented by a set of differential equations with t denoting time, t_o the initial time, as shown in Eq.(1):

$$\begin{cases} \dfrac{\partial \overline{\theta}(t)}{\partial t} = \overline{H}\left(\overline{\theta}(t), t\right) \\ \overline{\theta}(t_0) = \overline{\theta}_0 \end{cases} \tag{1}$$

In Eq.(1), $\bar{H}$ is a non-linear function of all the input and output parameters $\bar{\theta}(t)$, in general.

For many models which are used in practice, the time necessary to calculate the final state of a system can be prohibitive, especially when running a model many times to explore uncertainties. One solution which has been used to reduce the number of times it is necessary to sample a complex model for uncertainty quantification is the implementation of SMs. SMs use a small number of initial runs as training data to predict the response throughout the remainder of the uncertainty space, as described in Eq.(2)

$$\Theta(\bar{\theta}_0) \approx \bar{H}(\bar{\theta}_0). \tag{2}$$

where Θ represents the SM, and is designed to estimate the output of the model $\bar{H}$ for the same set of initial parameters. As this relationship no longer requires solving the full set of differential equations in Eq.(1), these SMs can be processed several orders of magnitude more quickly.

Since SMs do not contain any information about the true structure of the system model, their accuracy varies depending on the underlying structure of the FCM [7]. The determination of this underlying structure is complex and presents a large additional burden on analysts attempting to take advantage of SMs.

Some SMs return only binary success/fail results. These models, described as classifiers, operate in the uncertainty space transformed by a goal function, which defines success or failure. The goal function used in this paper, which is failure of NSCs that undergo acceleration greater than the failure acceleration for a given run, is shown in Eq.(3)

$$C_{NSC} = \begin{cases} 0 \; if \; a_{NSC} < f_{NSC} \\ 1 \; if \; a_{NSC} \geq f_{NSC} \end{cases} \tag{3}$$

where C_{NSC} represents the output of the model $\bar{H}$ after being transformed into the binary success/failure domain for an NSC, a_{NSC} is the acceleration of the NSC and f_{NSC} is the failure acceleration obtained using Table 1.

For this study, several SMs were investigated including [8]:

- K-Neighbors Regressor
  - K=1 (NNR) and K=5 (5NR)
- K-Neighbors Classifier
  - K=1 (NNC) and K=5 (5NC)
- Inverse Distance Weighting (IDW)
- Linear Support Vector Classifier (L-SVC)
- C-Support Vector Classifier (C-SVC)

The K-Neighbors SM uses a set of training points as a library for further polling. After constructing this library of data points and their outputs, points within the uncertainty space can be chosen for sampling on the SM. For each of these sampling points, the K nearest to the sampling point that are stored in the library are selected and their outputs are averaged, with the mean value of the selected points' outputs given as the output of the SM.

IDW [9] models also create a library of training data and polls their distances from a sampling point. However, IDW models base their estimate on all of the training points, applying weighting determined by the inverse of the distance from the sampling point to the training points, represented in Eq.(4):

$$\Theta\left(\overline{\theta}_s\right) = \frac{\sum \frac{\overline{H}\left(\overline{\theta}_i\right)}{\left(\overline{\theta}_s - \overline{\theta}_i\right)^p}}{\sum \left(\overline{\theta}_s - \overline{\theta}_i\right)^p} \tag{4}$$

In Eq.(4), $\overline{\theta}_s$ represents the initial state of the model parameters for the SM, while $\overline{\theta}_i$ represents the state of model parameters for the i[th] training run.

Both L-SVC and C-SVC models are classifiers; they only attempt to distinguish success from failure of a system. L-SVC models construct a hyperplane through the uncertainty space which bisects it into regions of success and failure. By maximizing the distance between the hyperplane and the nearest training points, and minimizing the intrusion of failures or successes into the inappropriate region, the separation between these regions can be maximized.

C-SVC models also use a hyperplane to separate the uncertainty space, but can be generalized to nonlinear hypersurfaces. Conceptually this occurs by mapping the space to include an additional dimension. A hypersurface is drawn in this dimension and then transformed back to the original space, including the now nonlinear hypersurface. Practically, however, a kernel is used to replicate this nonlinear behavior without explicitly transforming the space.

3.1. SM Analysis

In the study presented in this paper, we use RAVEN to generate the FS and AS. To generate each set of data, a number of training points are created by sampling the uncertain parameters listed in Table 1: m_1, m_2, k_1 and k_2. Sampling employs LHS to explore the uncertainty space and use these sampled values in a single run of the seismic model, generating the peak accelerations of NSCs at Floors 1 and 2 (NSC_1 and NSC_2, respectively).

In the AS, a limited number of training runs are performed (see Section 3.2). These results are then used to train the SMs listed in Table 2. Regressor SMs are trained on the input parameters of m_1, m_2, k_1, and k_2 and the output acceleration parameters for NSC_1 and NSC_2. The classifiers are trained using a success/fail parameter instead of the peak acceleration. As these SMs do incorporate the failure acceleration (see Table 1), the input parameters are expanded to include the sampled value of the failure acceleration along with m_1, m_2, k_1, and k_2. The outputs of the classifiers used for training are the success or failure of NSC_1, NSC_2, or their failure jointly (NSC_J).

Table 2. SMs used for analysis and their trained parameters of interest.

SM	Training parameter
NNR	Peak Acceleration
5NR	Peak Acceleration
IDW Regressor	Peak Acceleration
NNC	Success/Failure
5NC	Success/Failure
IDW classifier	Success/Failure
L-SVC	Success/Failure
C-SVC	Success/Failure

The models in Table 2 are themselves sampled 10,000 times each and for each SM, the probabilities for failure for NSC_1, NSC_2, and NSC_J are calculated. The relative errors between each SM and the

highest-fidelity set of training runs within the AS are found. We repeat this process, using a larger number of training runs, until the most accurate SM reaches convergence.

For the FS, 20,000 samples of the FCM are performed to determine the probability of failure of NSCs. The probabilities of failure for NSCs calculated by the FS are compared to the results from SMs trained using data from the AS and the most accurate SM is identified.

3. RESULTS

In this section, the details of the seismic model, as found by the FS, are given in Section 3.1. The results of the AS are detailed in Section 3.2, and the comparison between the FS and the AS is provided in Section 3.3.

3.1. FS Analysis

NSC accelerations from seismic events are an important failure mechanism because this represents a way for otherwise-isolated systems to suffer simultaneous failures, based on their physical proximity within the same NPP. In this analysis, both NSC1 and NSC2 are located in the same structure. Therefore their movements are correlated, and because the auxiliary building is not fully rigid, higher floors sway more than lower floors. This correlation leads to NSC2 generally having a greater peak acceleration than NSC1, as shown in Fig.2, which illustrates the peak accelerations experienced by both NSCs. In Fig.2, points shown in blue represent cases where NSC2 had a greater peak acceleration than NSC1. The points shown in red represent cases where NSC1 had a greater peak acceleration. These red points are located in the lower-right section of Fig.2, and are most visible with a peak acceleration of NSC1 between 0.5 and 2g.

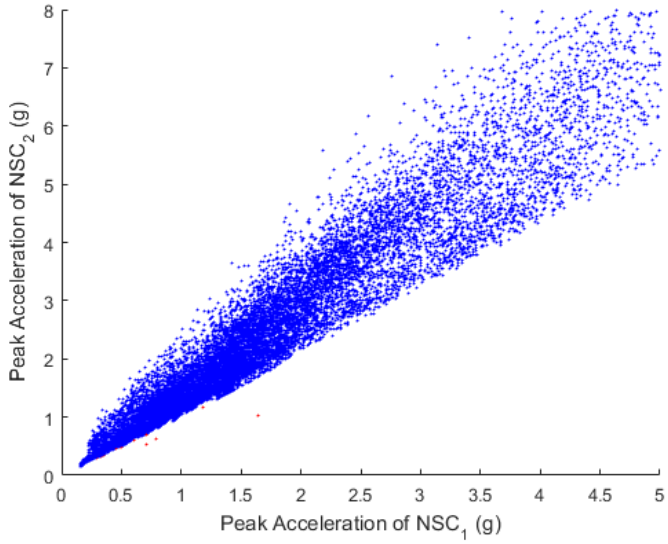

Fig.2. Seismic accelerations of NSC1 and NSC2, based on the Full Set Analysis, capped at 5g for NSC1 and 8g for NSC2.

The conditional failure probabilities for NSC1 and NSC2 are based on the peak accelerations located in Fig.2. For each run, the accelerations of NSC1and NSC2 are compared to the failure acceleration drawn from the uncertain distribution outlined in Table 1. If the experienced acceleration exceeds the failure acceleration, the NSC is considered to have failed. The failure probabilities are given in Table 3.

Table 3. Conditional failure probabilities of NSCs based on the Full Set Analysis.

F_{P1} (NSC_1 | GM_S)	F_{P2} (NSC_2 | GM_S)	F_{PJ} ($NSC_1 \cap NSC_2$ | GM_S)
0.6109	0.7094	0.6109

For simplicity in illustration, both NSCs are assumed to be identical. As such, a single sample of the failure acceleration limit applies to both NSCs. Given that the acceleration experienced by NSC2 in Fig.2 are almost uniformly greater than those experienced by NSC1, as shown by the dominance of blue points to red points, the joint failure probability is identical to the NSC2 failure probability, which implies that there were no instances during this simulation where NSC2 survived a seismic event that failed NSC1.

Seismic behaviors are often difficult to predict because the responses of structures depend heavily on their resonance frequencies, which are driven in large parts by the masses and stiffnesses of different sections of the structure. As mass and stiffness are uncertain within this analysis, the resulting NSC successes and failures do not map cleanly into the uncertainty space, as Fig.3 shows. Instead the response appears to create several small pockets of success or failure. As many SMs, such as L-SVC models, attempt to divide the input space cleanly into regions of success and failure, these models will likely have great difficulty representing this problem, while more local SMs will be better able to reconstruct this output.

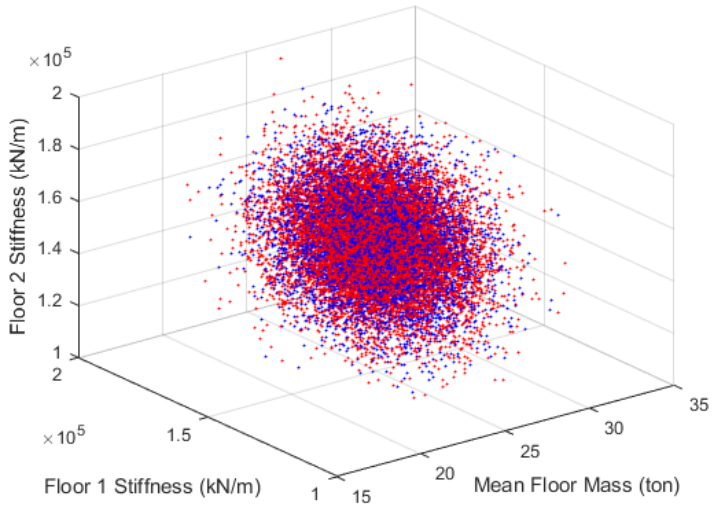

Fig.3. Input values of the stick model and NSC response. Points in blue include success of either NSC, while points in red correspond to the joint failure of both NSCs. Note that both m1 and m2 have been combined into the mean floor mass parameter and that the failure acceleration threshold is not shown.

3.2. AS Analysis

AS consists of several sets of samples where LHS is used to generate training data. These start at 250 training samples and increase to convergence, following the progression listed in Table 4. Using these training sets, the series of SMs are then constructed to either return the peak accelerations of both NSCs for those models which output peak acceleration, as described in Table 2, or the joint probability of failure P_J for classifier models, again described in Table 2. These results are included in Table 4.

The failure probabilities for these SMs vary widely. To provide a baseline to determine suitable SMs, the probability of NSC_J failure from each SM is compared to the probability of failure calculated by that SM's training data. Using Eq.(5), the relative error of a SM is calculated and included in Table 4:

$$E_{PJ}(i) = \frac{\left|A_{PJ}(i) - B_{PJ}(i)\right|}{B_{PJ}(i)} \tag{5}$$

In Eq.(5), $B_{PJ}(i)$ is the probability of failure from training data consisting of i runs and A_{PJ} is the probability of failure from a SM trained on these data.

From the data in Table 4, we see that the relative error of different SMs can be separated into several categories. Two SMs, the NNR and the IDW Classifier models, have small relative errors and match the seismic model well. Beyond that are the IDW Regressor and the 5NR models, which settle down to a consistent error that is unacceptably high. Worse than those are the NNC, 5NC and L-SVC models, which have relative errors that jump wildly based on the number of training runs. Finally, the C-SVC model quickly pegs itself to 100% relative error. This is illustrated in Fig.4.

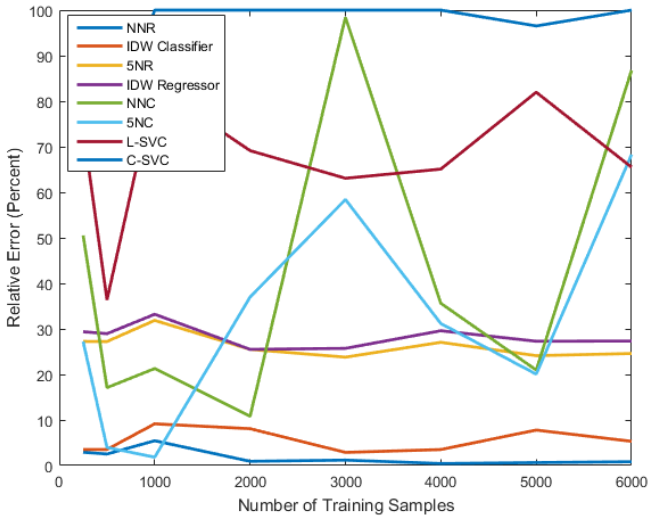

Fig.4. Relative errors for each SM.

Using the relative errors in Fig. 4, it is clear that the NNR model best represents the training data. However, this is not sufficient to determine if the SMs have converged. To determine if SMs have converged, it is necessary to use the failure probabilities directly. Based on the results illustrated in Fig.4, the NNC, 5NC, L-SVC and C-SVC models vary wildly or have such large persistent errors that little to no information about the failure rate of NSC_J can be extracted. Therefore, they were neglected for further analysis and the failure probabilities for the remaining SMs are illustrated in Fig.5.

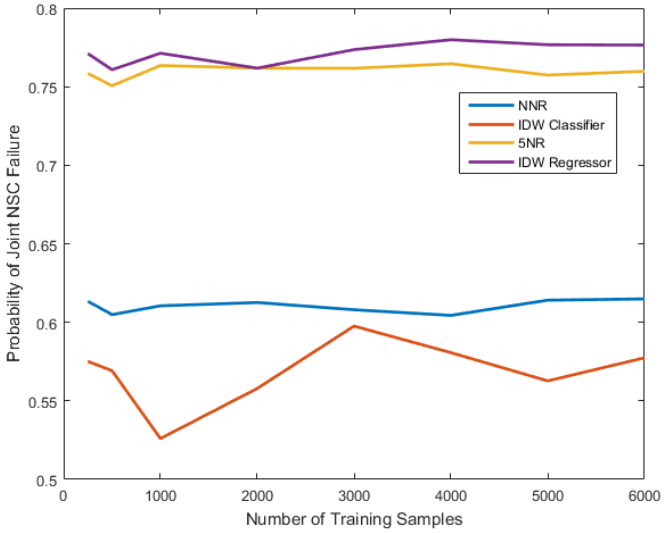

Fig.5. Joint NSC failure probability for selected SMs.

From Fig.5 it is possible to begin drawing conclusions about the convergence of these SMs. The NNR model appears to have converged by 5,000 training points, which is also true for the 5NR and IDW Regressor models. The IDW Classifier does not reach convergence within the scope of this analysis. From Fig.5, it is clear that the NNR SM still provides the best estimate of the seismic model results.

Table 4. Conditional failure probabilities of NSC_J based on surrogate models and errors in failure probability based on the number of training runs, defined in Eq.5.

TRAINING RUNS / SURROGATE MODEL		B_{PJ}	IDW REGRESSOR	NNR	5NR	IDW CLASSIFIER	NNC	5NC	L-SVC	C-SVC
250	A_{PJ}	0.5960	0.7711	0.6134	0.7584	0.5751	0.2948	0.7583	0.1543	1
	E_{PJ}		29.38%	2.919%	27.25%	3.507%	50.53%	27.23%	74.11%	67.79%
500	A_{PJ}	0.5900	0.7608	0.6049	0.7506	0.5692	0.6909	0.6134	0.3754	1
	E_{PJ}		28.95%	2.525%	27.22%	3.525%	17.10%	3.97%	36.37%	69.49%
1000	A_{PJ}	0.5790	0.7713	0.6105	0.7635	0.526	0.4557	0.5896	0.0963	0
	E_{PJ}		33.21%	5.440%	31.87%	9.154%	21.30%	1.83%	83.37%	100%
2000	A_{PJ}	0.6070	0.7618	0.6126	0.7618	0.5579	0.5414	0.3825	0.1873	0
	E_{PJ}		25.50%	0.922%	25.50%	8.09%	10.80%	36.99%	69.14%	100%
3000	A_{PJ}	0.6153	0.7736	0.608	0.7617	0.5976	0.0098	0.2559	0.2272	0
	E_{PJ}		25.72%	1.186%	23.79%	2.877%	98.41%	58.41%	63.07%	100%
4000	A_{PJ}	0.6018	0.7799	0.6044	0.7646	0.5807	0.8162	0.7894	0.2101	0
	E_{PJ}		29.59%	0.432%	27.05%	3.506%	35.63%	31.17%	65.09%	100%
5000	A_{PJ}	0.6102	0.7767	0.6141	0.7574	0.5627	0.4823	0.4878	0.1100	0.0212
	E_{PJ}		27.29%	0.639%	24.12%	7.78%	20.96%	20.05%	81.97%	96.53%
6000	A_{PJ}	0.6098	0.7765	0.6149	0.7598	0.5774	0.0805	0.1934	0.2104	0
	E_{PJ}		27.33%	0.836%	24.60%	5.31%	86.80%	68.28%	65.49%	100%

3.3. FS Comparison With AS

Since the FS data from Section 3.1 represent our most complete understanding of the system, they are used as the basis for comparison for SMs trained using the AS.

In Table 3, NSC_J failure probability from the FS data is shown to be 0.6109. This result, constructed from a high-fidelity sample of the original seismic model, is the goal for the SMs to match. The errors of each SM using 6,000 training points (see Table 4) with respect to F_{PJ} in Table 3 are listed in Table 5. From these results it is clear that the most accurate SM was the NNR model, with a relative error of less than 1%. (0.08% from Table 5)

To determine if the SMs are truly converged based on the number of training points, each SM was then trained using the 20,000 points that make up the FS. If a SM has converged with respect to the number of training points, the SM with 20,000 training points should give similar probabilities of failure as the SM results from Section 3.2. Table 5 includes the relative error of SMs trained with the FS. These results confirm that the NNR model had reached convergence after being trained on the AS with 6000 data points since the relative error is 0.57%. The IDW Regressor and 5NR models also converged (relative error 0.63% and 0.30%, respectively) using data from the AS, but reached predictions that had an unacceptably large error with respect to F_{PJ} in Table 3 (27.9% and 24%, respectively). The IDW Classifier model was more accurate (4.57% error with respect to F_{PJ} in Table 3) than either the IDW Regressor or 5NR models, but this model did not reach convergence within the AS data (see Fig.5) and was less accurate than the NNR model, having 4.57% error with respect to F_{PJ} in Table 3 compared to 0.08% corresponding error of NNR model. Based on the analysis in Section 3.2, the remaining models were not determined to have converged.

Table 5. Relative error A_{PJ} (Section 3.2) of SM Trained with 6000 Runs

Compared to	**IDW Regressor**	**NNR**	**5NR**	**IDW Classifier**	**NNC**	**5NC**	**L-SVC**	**C-SVC**
F_{PJ} in Table 3	27.91%	0.08%	24.00%	4.57%	12.56%	16.65%	62.45%	88.71%
SM trained using 20,000 run FS data	0.63%	0.57%	0.30%	0.96%	88.29%	72.86%	8.28%	100%

4. CONCLUSION

SMs have seen use in several industrial applications, as they can reduce the number of runs an analysis needs to perform on a computer model. For nuclear applications, this is often of great importance because many nuclear models are characterized by long run times. However, the selection of an appropriate SM is a challenging task that can often require a thorough understanding of the system's behavior. Instead, we performed an increasing amount of sampling on a wide variety of SMs, in order to find which models performed well in this system and gain an understanding of how many training runs were required for the SMs.

We have found that for the system under consideration, the NNR model was able to best match the system (0.08% compared to the F_{PJ}-see Table 5), reaching convergence within 5,000 training samples (see Fig.5), compared to the 20,000 required for the FS. The IDW Classifier was the second-most accurate model (4.57% error with respect to F_{PJ} by Table 5), but converged more slowly than the NNR (see Section 3.2). The other models considered in this analysis were quickly determined to have very little predictive capabilities. Further work remains in expanding this methodology to different computer models and seeking new strategies to further reduce the number of necessary training runs.

References

[1] D. Gaston, C. Newman, G. Hansen and D. Lebrun-Grandie, “MOOSE: A Parallel Computational Framework for Coupled Systems of Nonlinear Equations,” Nuclear Engineering and Design, 239(10) (October 2009).
[2] A. Alfonsi, C. Rabiti, D. Mandelli, J. Cogliati and R. Kinoshita, “RAVEN As a Tool for Dynamic Probabilistic Risk Assessment: Software Overview,” INL/CON-13-28291, Idaho National Laboratory, Idaho Falls, ID (May 2013).
[3] J. Hur, A. Guler, H. Sezen, T. Aldemir and R. Denning, “Assessment of Conservatism in the Separation of Variables Approach to Seismic Probabilistic Risk Assessment,” 2016 International Congress on Advances in Nuclear Power Plants, San Francisco (CA) 2016.
[4] B. Cohn, R. Denning, T. Aldemir, J. Hur and H. Sezen, “Implementation of SMs within RAVEN to Support SPRA Uncertainty Quantification” in 2017 European Safety and Reliability Conference, Portorož (Slovenia) 2017.
[5] B. Cohn, R. Denning, T. Aldemir, J. Hur and H. Sezen, “SM Selection in RAVEN for Seismic Dynamic PRA/PSA” in 2017 International Topical Meeting on Probabilistic Safety Assessment and Analysis, Pittsburgh (PA) 2017.
[6] B. Ellingwood, “Issues related to structural aging in probabilistic risk assessment of nuclear power plants.” Reliability Engineering & System Safety, 62.3 (1998): 171 – 183
[7] A. Forrester, A. Keane, “Recent Advances in Surrogate-Based Optimization.” Progress in Aerospace Sciences, vol. 45 (2009), pp. 50-79
[8] A. Alfonsi, C. Rabiti, D. Mandelli, J. Cogliati, C. Wang, P. Talbot, D. Maljovec and C. Smith, “RAVEN Theory Manual,” INL/EXT-16-38178, Idaho National Laboratory, Idaho Falls, ID (March 2016).
[9] N. Lam, “Spatial Interpolation Methods: A Review,” The American Cartographer, vol. 10.2, (1983).
.